Predicting Near-Field Specific Impulse Distributions using Machine Learning

J.J. Pannell[a], S. E. Rigby[a], G. Panoutsos[a], A. Tyas[a], S.B. Cooke[b], D.J. Pope[b]

[a] University of Sheffield, Mappin Street, Sheffield, S1 3JD, UK

[b] Defence Science and Technology Laboratory (Dstl), Porton Down, Salisbury, Wiltshire, SP4 0JQ, UK

INTRODUCTION AND CONTEXT

High-fidelity physics modelling methods, such as those used within hydrocodes, can accurately simulate blast-load development on a variety of complex structures. These approaches require considerable computation effort and so are unsuitable for undertaking platform survivability assessments where structural response to a large range of blast loading configurations must be considered. The blast protection community is equipped with well-established, quick-running engineering tools, such as the Kingery and Bulmash semi-empirical method [1] that allows for rapid evaluation of blast wave parameters from a given explosive event. These methods are unsuitable, however, when considering different shapes of explosives, and/or those located extremely close to a structure where complex interactions between the explosive and target result in a highly spatially non-uniform loading. Experimental work undertaken by Rigby et al. [2] highlights the complexity of this extreme near-field loading, and outlines the requirement for this complexity to be considered when predicting subsequent structural response [3].

Machine learning techniques have been shown to accurately predict peak overpressures and peak scaled impulses in complex environments [4], specifically behind blast walls [5] and in simple city street scenarios [6]. These approaches utilise computational fluid dynamics (CFD) analyses, and occasionally experimental data, to provide training data for a machine learning framework that implicitly learns the relationship between input and output. This is particularly useful when the relationship is complex and not known explicitly. This results in fast-running predictive models that can provide peak impulses and overpressures within the boundaries of the trained database to produce predictive information about likely injury and damage levels. These methods fall short, however, in that they do not provide a characterisation of the loading, used to inform structural response, in a more accurate manner whilst still retaining the computational efficiency of semi-empirical methods once the model itself is trained.

There is, therefore, a need for a fast-running model that can provide crucial load characterisation information. This paper presents a machine learning framework that accurately predicts specific impulse distributions for extremely near-field scenarios (within the boundaries of the training database) from a given feature, stand-off.

NEAR-FIELD VALIDATION OF *APOLLO BLASTSIMULATOR*

Introduction

Apollo blastsimulator is a CFD tool developed by the Ernst-Mach-Institut that specialises in the simulation of high-dynamic flow problems. In this paper *Apollo blastsimulator* has been used to provide the training data for the machine learning framework. To validate *Apollo blastsimulator* in extreme near-field scenarios, it was compared to experimental data collected by Rigby et al. [2] at the University of Sheffield and ConWep/Kingery & Bulmash [1] output.

Experimental Setup

Blast load distributions were measured in experiments conducted at the University of Sheffield Blast & Impact laboratory in Buxton, UK using the Characterisation of Blast Loading (CoBL) apparatus (experimental set up is shown in Figure 1). It comprises a pair of stiff, massive fibre and bar reinforced concrete frames spaced 1m apart, with each frame comprising two 500mm square columns with a 750mm deep, 500mm wide concrete beam spanning horizontally between the two columns. A 100mm thick steel target plate is underslung from the soffits of the horizontal beams and acts as a nominally rigid boundary to reflect the shock wave and detonation products impinging on the target after detonation of an explosive some distance beneath the centre of the plate. The plate is 1.4m in diameter to negate the effect of blast wave clearing around the target edge [7].

The target plate is drilled through its thickness to allow 10mm diameter, 3.25m long EN24(T) steel HPBs to be mounted and set with their loaded faces flush with the underside of the target plate. A total of 17 bars were used; one central bar and four bars located at each radial offset of 25, 50, 75 and 100mm from the plate centre, with the bar naming convention following the coordinate axes shown in Figure 1(**b**).

Kyowa KSP-2-120-E4 semi-conductor strain gauges were mounted in pairs on the perimeter of each HPB at 250mm from the loaded face, in a Wheatstone-bridge circuit to neglect any bending effects and to ensure that only the axial strain component was recorded. Strain data were recorded using 14-Bit digital oscilloscopes at a sample rate of 3.125MHz and were triggered via a voltage drop in a separate breakwire channel.

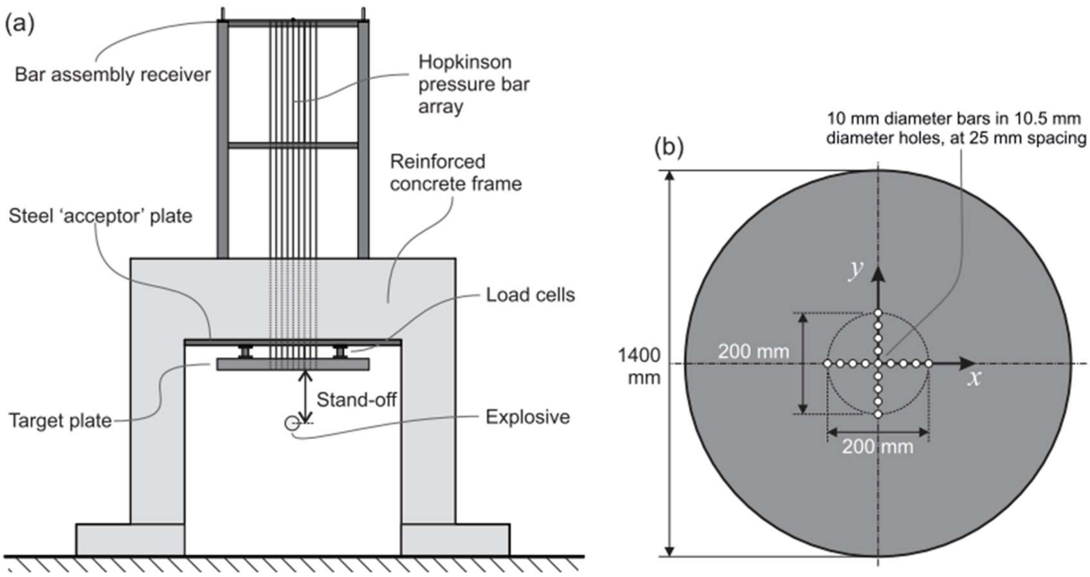

Figure 1 – Schematic of UoS testing apparatus (not to scale): (**a**) elevation; (**b**) detailed plan view of target plate showing bar arrangement and coordinate axes. Image taken from [2].

Comparison to *Apollo blastsimulator*
Three experimental repeats were obtained by Rigby et al. [2] for two spherical charge scenarios: 80mm standoff and 380mm standoff, both with a spherical charge mass of 100g PE4, totalling six available tests for comparison (with 17 measurement locations per test). The geometry of the *Apollo blastsimulator* CFD analyses is shown in Figure 2, overall domain sizes are 0.5m x 0.5m x 0.5m, zone length of 20mm with a resolution level of 4, leading to an ultimate zone length of 1.25mm. 1D to 3D mapping was used via the B1D module in *Apollo* to extend the 1D domain to one complete zone length away from the rigid boundary. This model information was informed by a mesh sensitivity analysis that has been omitted for brevity.

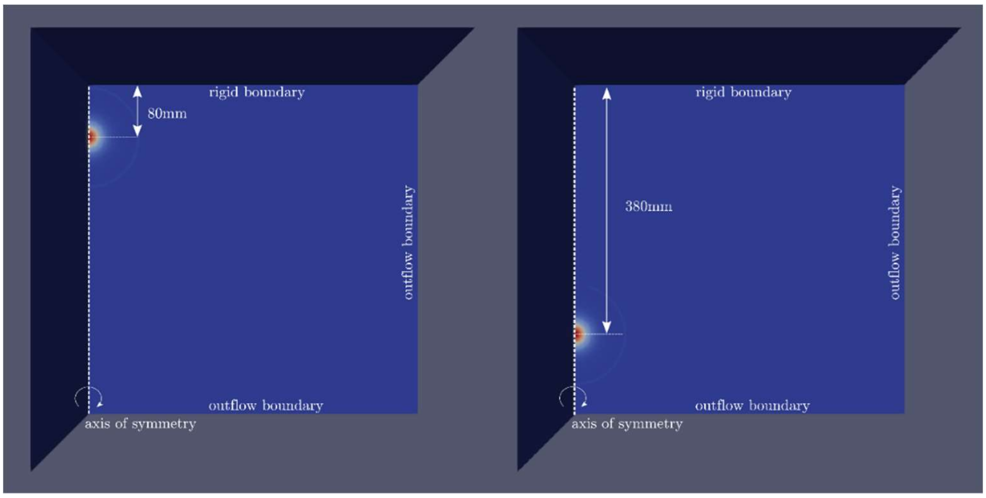

Figure 2 - Geometry of spherical 100g charge scenarios modelled in *Apollo blastsimulator*. 80mm standoff (left) and 380mm standoff (right).

Considering data from the 80mm stand-off tests, shown in Figure 3, it can be seen that there is a good agreement in peak overpressures, impulses, and overall pressure histories. *Apollo* simulation output has not been manipulated for arrival time which shows a slight delay to experimental data.

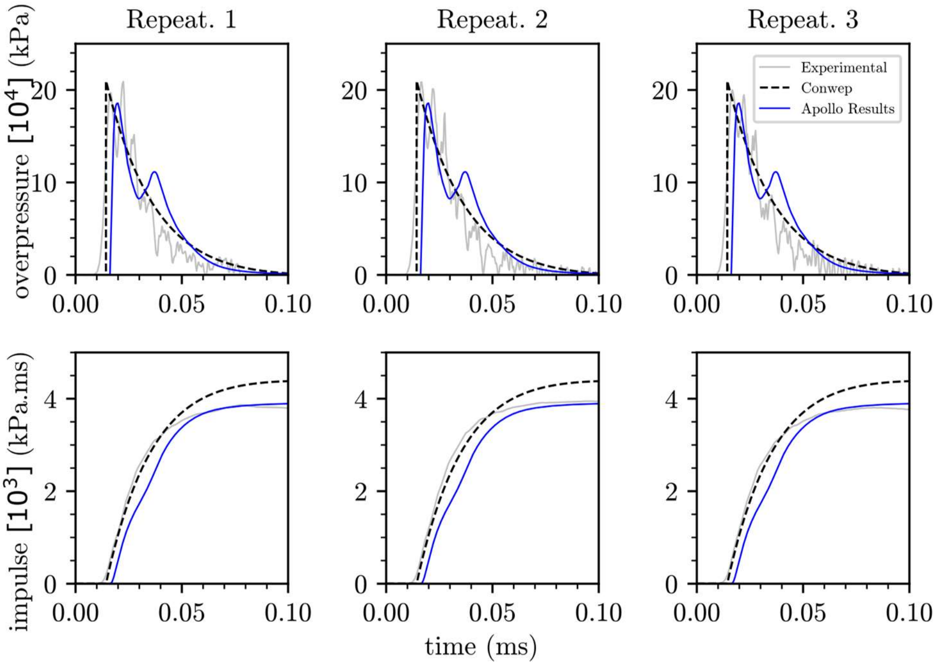

Figure 3 - Overpressure/impulse time histories for 100g PE4 at 80mm stand-off.

Results from the 380mm stand-off experiments and simulations are show in Figure 4. Peak overpressures here generally are more accurate than in the 80mm instance. Peak impulse, however, is less accurate than the 80mm scenario, albeit still within the range of ConWep and experimental results.

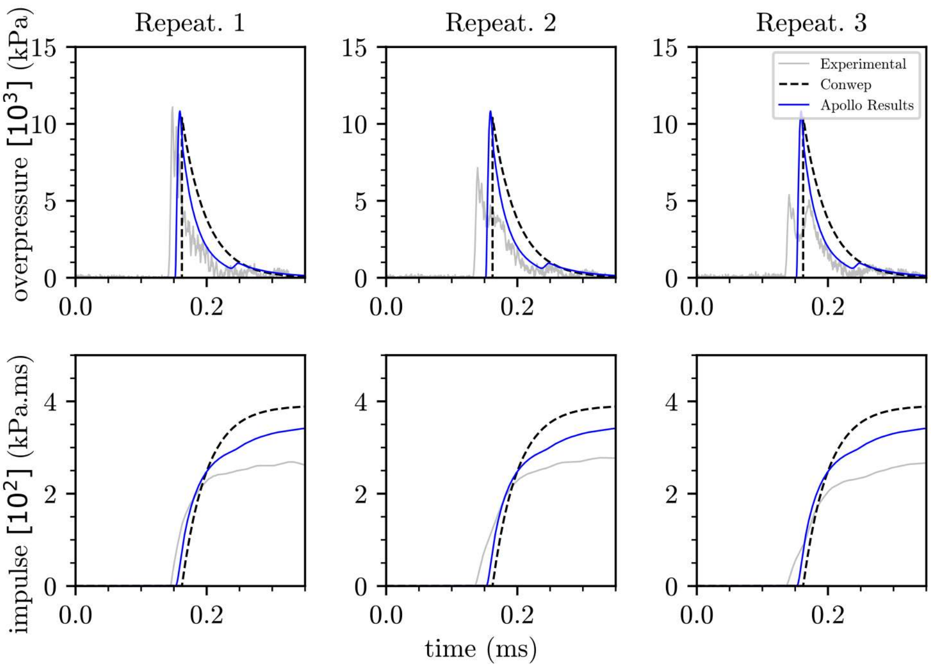

Figure 4 - Overpressure/impulse time histories for 100g PE4 at 380mm stand-off.

Specific impulse distribution profile comparison

Whilst peak pressure may need to be considered for longer duration loading relative to the natural period of the structure, the distribution of peak specific impulse is the primary parameter which dictates structural response (e.g. [2,3]). The CoBL apparatus is able to determine this loading distribution through temporal integration of the pressure signals recorded at various distances along the target. This setup was replicated in the *Apollo blastsimulator* CFD analyses by placing gauges along a length of wall, as in the schematic in Figure 5.

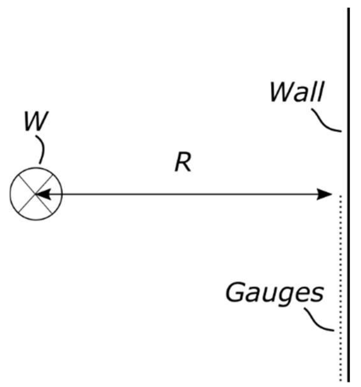

Figure 5 - Model set up to capture specific impulse distribution.

By recording the time histories at each gauge and plotting the peak specific impulse against distance one can obtain the specific impulse distribution of an explosive scenario. These distributions were compared to CoBL experimental data and are shown in Figure 6. As expected, as the standoff increases the peak specific impulse distribution becomes more uniform. *Apollo blastsimulator* shows good agreement in capturing the peak specific impulse distribution profiles and can be considered to provide valid training data for later analyses.

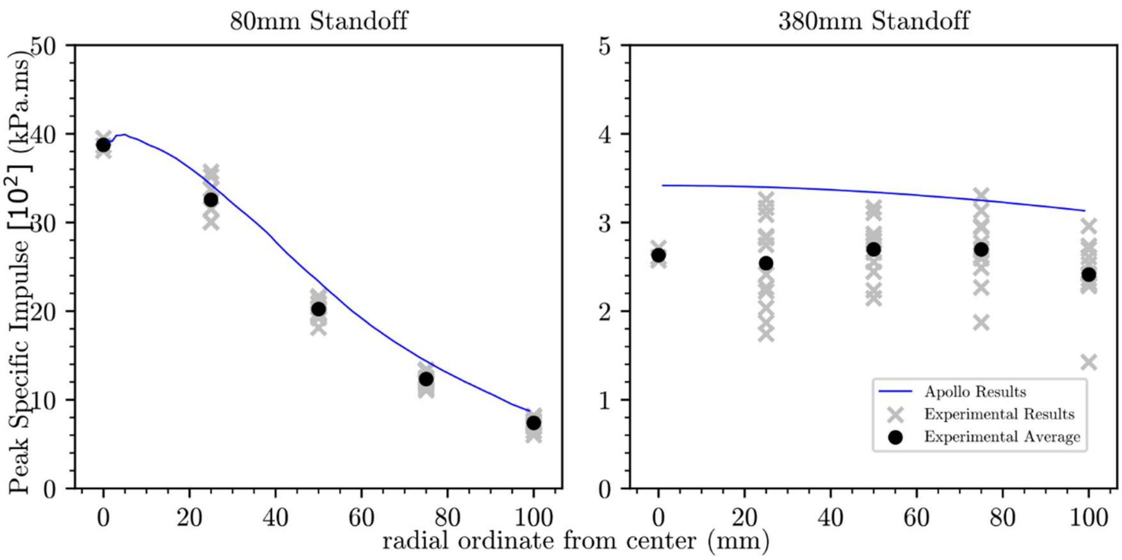

Figure 6 - Specific impulse distributions for 100g PE4 at 80mm and 380mm standoffs.

MACHINE LEARNING FRAMEWORK

Overview

The following section demonstrates the machine learning framework that has been created to predict peak specific impulse distribution from a feature, stand-off. This paper has previously validated the use of *Apollo* for providing accurate peak specific impulse distributions, therefore training data will be provided by these CFD analyses. As mentioned in the introduction, fast running predictive engineering models that provide important and accurate information about near-field loading are of interest to the blast research community.

This paper presents a framework where the user can input a value for stand-off (within a specified range of the training data) and it will return a peak specific impulse distribution. This framework is general and can apply to a larger range of training data and can be extended to investigating other features (e.g. explosive type, shape, etc.).

The overall workflow is shown in Figure 7, but the philosophy can be summarised as follows. The authors have used CFD peak specific impulse data where the only variable to change is stand-off. This data then undergoes a nonlinear regression where a function is fit to the CFD output. This process is repeated for each "sample" (as in each different stand-off), and the model now has knowledge of how the optimum parameters of a function vary with the feature (stand-off). Judgements are made by the authors on how to model the parameter-standoff relationships, and the chosen functions are fitted to this data, this provides a continuous function of optimum parameter vs. standoff, which allows the prediction of optimum parameters given a specified standoff.

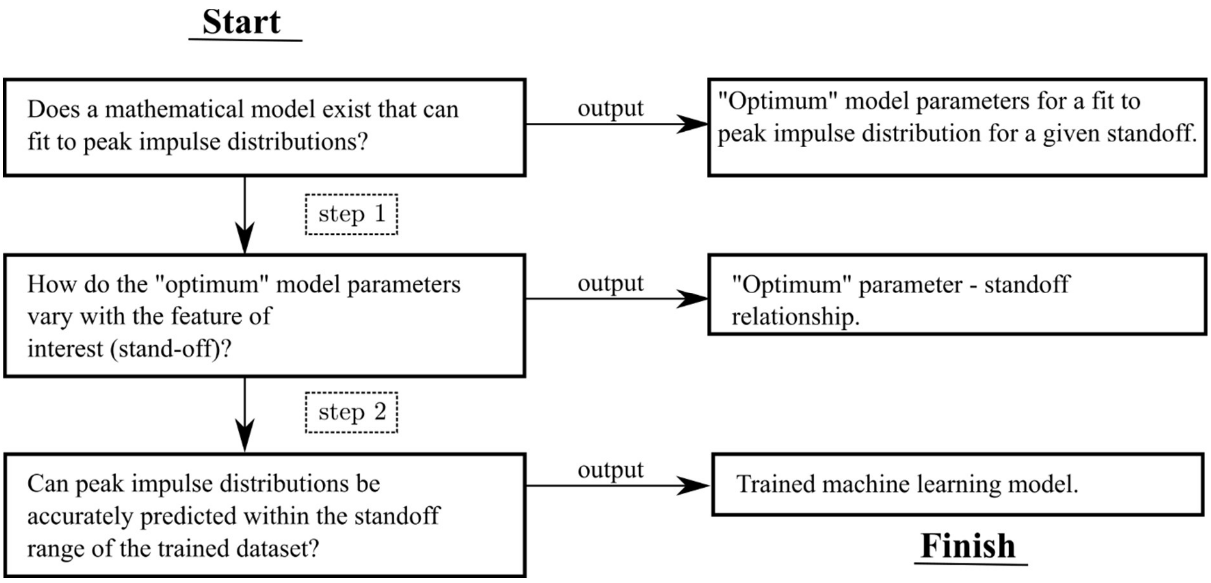

Figure 7 - Machine learning overall workflow.

Representation of peak specific impulse distribution and local fitting procedure - step 1 of workflow
Initially, we aimed to find a mathematical function that could represent the peak specific impulse distribution shape itself. By inspection of the shape of the peak specific impulse distribution, an initial decision to model the distributions with a Gaussian/bell-shaped family of functions was made.

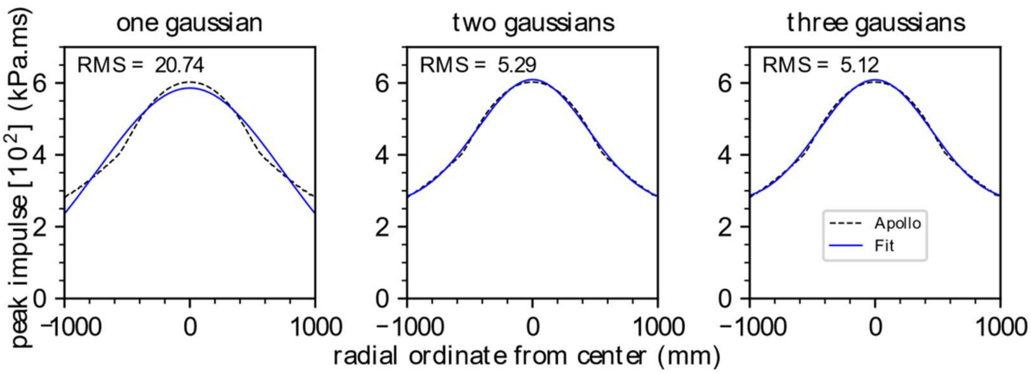

Figure 8 - Initial attempt fitting Gaussian functions to Apollo peak specific impulse distribution.

Figure 8 demonstrates the initial fitting of a Gaussian function (formula shown in Equation 1 below, where a is amplitude, b is centre and c is width) to *Apollo* peak specific impulse distributions. It consists of three separate functions, the first with one Gaussian, and the latter two with two or three Gaussian functions superposed respectively. The root-mean-square error ("RMS" on the plots) shows that both two and three Gaussians superposed are adequate to capture this distribution accurately. The two Gaussian model was taken forward as this is less complex (i.e. three less parameters) than the three Gaussian model.

$$f(\mathrm{x}) = a \times \exp\left(\frac{-(x-b)^2}{2c^2}\right) \tag{1}$$

The process of "fitting" the superposed Gaussian function to *Apollo* data is an optimisation problem, specifically a nonlinear regression. We first define a loss function, which is the objective function to be minimised, i.e. we minimise the error between the model and *Apollo* specific impulse distribution. The objective function to be minimised is the mean-squared-error of the model. We use a Trust Region Reflective algorithm as presented in [8] to perform this minimisation procedure and the output of this is the "optimum" Gaussian parameters for that sample.

The algorithm requires initial guesses to be made and allows the input of constraints between parameters. Preliminary fitting exercises showed the following constraints to be suitable (note: the subscript is indicative of the Gaussian it refers to, as the overall model is $\mathrm{Gaussian}_1$ added to $\mathrm{Gaussian}_2$)

$$a_1 > a_2$$

$$c_1, c_2 = 0.5$$

By setting up the constraints in this way, we allow the primary Gaussian to "dominate" the overall profile and the secondary Gaussian to "top-up" when additional complexity is required.

Global fitting procedure of entire dataset

Figure 9 demonstrates the overall procedure from initially running *Apollo* CFD analyses to the output of a dataset of predicted peak specific impulse distributions.

In the previous section we discussed the local fitting procedure of a Gaussian function to model peak specific impulse distribution. Having done this for all training samples, it is necessary to model the parameter-standoff relationships so that we can make predictions of parameter values from the standoff of the validation sample.

The two centre parameters are consistently set to 0.5, so do not require any fitting. The primary amplitude parameter is modelled as a decaying exponential with standoff, again using the Trust Region Reflective in [8]. The remaining amplitude parameter, and the two centre parameters are modelled as piecewise linear functions, using a differential evolution algorithm to define the breakpoints as in [9].

RESULTS

A training database of 20 samples were tested. The samples used 1kg TNT detonated at the following stand-off/scaled distances. Stand-off was set as logarithmically decaying with the base set as the charge radius. Note stand-off and scaled distance are interchangeable in these analyses as stand-off is set as multiples of charge radius.

Sample No.	Stand-off(m)	Sample No.	Stand-off(m)	Sample No.	Stand-off(m)	Sample No.	Stand-off(m)
1	0.230	6	0.357	11	0.555	16	0.863
2	0.251	7	0.390	12	0.606	17	0.943
3	0.274	8	0.426	13	0.662	18	1.030
4	0.299	9	0.465	14	0.723	19	1.125
5	0.327	10	0.508	15	0.790	20	1.229

Figure **10** shows the results of the *Apollo* simulations, the "optimum" model plots and the predicted peak specific impulse distribution. Figure 11 shows the parameter accuracy plots which provide a greater insight into model accuracy of individual parameters. Overall there is a strong agreement between model predictions from the machine learning framework and the *Apollo* simulations and this framework will provide an accurate fast running predictive method for predicting peak specific impulse distributions across the range of the dataset.

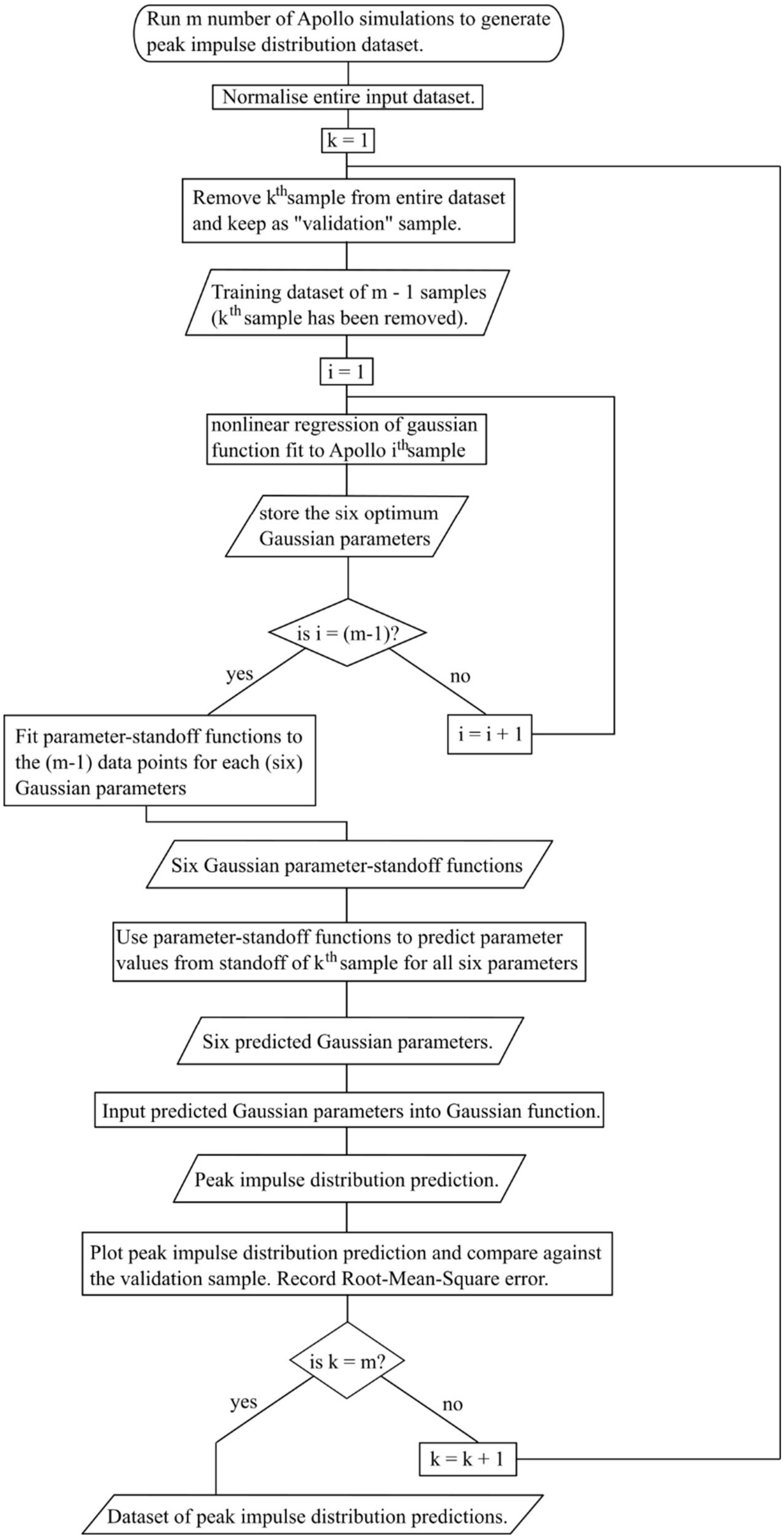

Figure 9 - Model fitting procedure

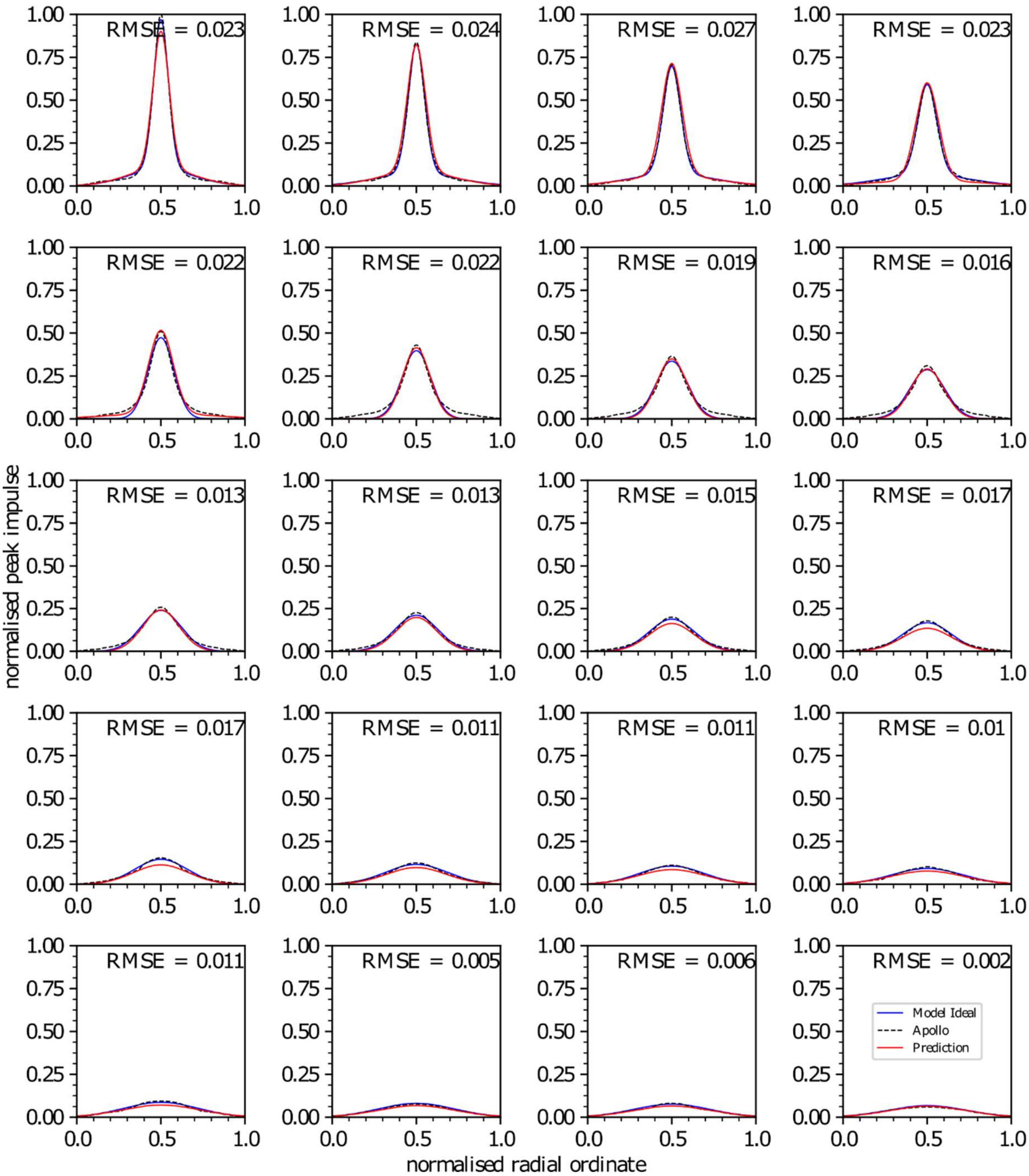

Figure 10 - Results of 20 Apollo samples of 1kg TNT at various scaled distance/stand-offs. Scaled distance/stand-off starting at top left at 0.23m/kg$^{1/3}$ and reading left to right finishing at 1.23 m/kg$^{1/3}$ bottom right.

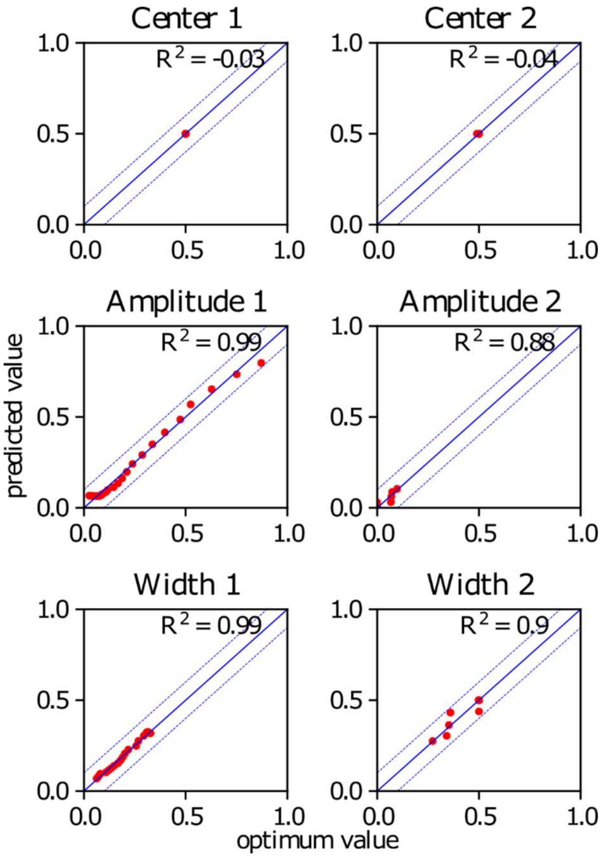

Figure 11 - Parameter accuracy plots (dotted lines indicate 10% prediction error either side)

SUMMARY AND OUTLOOK

In this work, we present a machine learning framework for calculating the distribution of specific impulse acting on a rigid surface following detonation of a spherical PE4 explosive located at a range of near-field stand-off distances. The results show that it is possible to develop a generalised framework populated by validated CFD training data and a number of simple constraints. Work of this nature presents two key opportunities. First, relationships between each Gaussian parameter and scaled distance can be extracted from the model, allowing for "offline" predictive equations to be derived from the modelling/machine learning approach. Although the process adopted here has been based on purely empirical datasets, the techniques could be transposed to develop prediction methods based on physical principles. Here, semi-empirical, dimensional analysis could be augmented to generate spatial distributions of specific impulse which are a direct function of parameters such as explosive type, charge shape and charge stand-off. Secondly, the blast load prediction techniques presented here can be linked to equivalent structural response algorithms (e.g. [3]) to provide an appropriately rapid and accurate means of platform survivability analysis.

REFERENCES

1. Kingery, C.N., Bulmash, G., "Airblast parameters from TNT spherical air burst and hemispherical surface burst," US Army BRI
2. Rigby, S.E., Tyas, A., Curry, R.J., Langdon, G.S., *Experimental Mechanics* 59:163-178 (2019).
3. Rigby, S.E., Akintaro, O.I., Fuller, B.J., Tyas, A., Curry, R.J., Langdon, G.S., Pope, D.J., *International Journal of Impact Engineering* 128:24-36 (2019).
4. Remennikov, A.M., Rose, T.A., *International Journal of Impact Engineering* 34:1907-1923 (2007)
5. Rose, T.A., Smith, P.D., Mays, G.C., *Proceedings of the Institution of Civil Engineers: Structures and Buildings*, pp78-85 (1995)
6. Remmikov, A.M., Mendis, P.A., *Design against Blast*, 60:1755-8336 (2012)
7. Rigby, S.E., Tyas, A., Bennet, T., Fay, S.D., Clarke, S.D., Warren, J.A., *International Journal of Protective Structures*, 5(3):253-274 (2014).
8. Branch, M.A., Coleman, T. F., Li, Y., *SIAM Journal on Scientific Computing*, 21(1):1-23 (1999).
9. Storn, R., Price, K., *Journal of Global Optimization*, 11(4):341-359 (1997).